

MicroRNA-200c mitigates invasiveness and restores sensitivity to microtubule-targeting chemotherapeutic agents

Dawn R. Cochrane, Nicole S. Spoelstra, Erin N. Howe, Steven K. Nordeen, and Jennifer K. Richer

Department of Pathology, University of Colorado Denver School of Medicine, Aurora, Colorado

Abstract

The transcription factor ZEB1 is normally not expressed in epithelial cells. When inappropriately expressed in carcinomas, ZEB1 initiates epithelial to mesenchymal transition due to its ability to repress E-cadherin and other genes involved in polarity. Recently, ZEB1 and ZEB2 have been identified as direct targets of the microRNA-200c family. We find that miR-200c levels are high in well-differentiated endometrial, breast, and ovarian cancer cell lines, but extremely low in poorly differentiated cancer cells. Low or absent miR-200c results in aberrant expression of ZEB1 and consequent repression of E-cadherin. Reinstatement of miR-200c to such cells restores E-cadherin and dramatically reduces migration and invasion. Microarray profiling reveals that in addition to ZEB1 and ZEB2, other mesenchymal genes (such as *FN1*, *NTRK2*, and *QKI*), which are also predicted direct targets of miR-200c, are indeed inhibited by addition of exogenous miR-200c. One such gene, class III β -tubulin (*TUBB3*), which encodes a tubulin isotype normally found only in neuronal cells, is a direct target of miR-200c. This finding is of particular significance because we show that restoration of miR-200c increases sensitivity to microtubule-targeting agents by 85%. Because expression of *TUBB3* is a common mechanism of resistance to microtubule-binding chemotherapeutic agents in many types of solid tumors, the ability of

miR-200c to restore chemosensitivity to such agents may be explained by its ability to reduce *TUBB3*. Because miR-200c is crucial for maintenance of epithelial identity, behavior, and sensitivity to chemotherapy, we propose that it warrants further investigation as a therapeutic strategy for aggressive, drug-resistant cancers. [Mol Cancer Ther 2009;8(5):1055–66]

Introduction

We previously reported that the transcription factor ZEB1 (zinc finger E-box binding homeobox 1; also known as TCF8, ZFH1A, ZFHEP, AREB6, BZP, NIL-2-A, and δ EF1) is aberrantly expressed in type 2 endometrial cancers that have undergone an epithelial to mesenchymal transition (EMT; refs. 1, 2). ZEB1 binds to E-box like sequences (CACCTG) and is involved in the development of mesodermal and neural tissues. ZEB1 and ZEB2 (SIP1) play a role in EMT during tumor progression by directly repressing E-cadherin (3–5) and other epithelial markers (6, 7). Endometrial cancers can be divided into two subtypes. Type 1 endometrial cancers (low-grade endometrioid adenocarcinomas) retain many epithelial characteristics and are relatively nonaggressive. In contrast, type 2 endometrial cancers are a heterogeneous group of poorly differentiated tumors (International Federation of Gynecology and Obstetrics grade 3 endometrioid adenocarcinomas, serous papillary, clear cell, and malignant mixed Müllerian tumors) with advanced stage at diagnosis and poor prognosis as compared with type 1 tumors (8, 9). Type 2 tumors often have lost epithelial markers and gained mesenchymal characteristics, and this affects their clinical behavior (aggressiveness). Some have suggested that a similar classification for ovarian cancers would be useful (10–12).

Recent research has implicated microRNAs (miRNA), acting as oncogenes and tumor suppressors, in the development and progression of cancers (13, 14). Many miRNAs localize to fragile sites and are frequently lost in cancer (15). Recently, it was reported that miR-200c targets *ZEB1* (16). It was later shown that other members of the miR-200 family, which share sequence homology, can target both *ZEB1* and the closely related gene, *ZEB2* (17, 18). These recent data suggest that the miR-200 family is responsible for maintenance of the epithelial phenotype, at least partially via repression of *ZEB1* and *ZEB2*. Indeed, we show that miR-200c expression is strongly associated with a more benign, less aggressive phenotype in endometrial, ovarian, and breast cancer cell lines. Levels inversely correlate with *ZEB1* and positively correlate with E-cadherin. We show that restoration of miR-200c expression to cancer cells that lack it suppresses *ZEB1* expression, thereby completely

Received 11/5/08; revised 2/5/09; accepted 2/14/09; published OnlineFirst 5/12/09.

Grant support: Department of Defense Breast Cancer Research Program Idea Award BC084162, Career Development Award (National Cancer Institute Cancer Center Support Grant P30-CA046934) from M. D. Anderson Uterine Specialized Program of Research Excellence grant CA098258 NIH/National Cancer Institute, The Avon Foundation, and Department of Pathology start-up funds (J.K. Richer). D.R. Cochrane was supported by a Thorikildsen Research Fund Endowment.

The costs of publication of this article were defrayed in part by the payment of page charges. This article must therefore be hereby marked *advertisement* in accordance with 18 U.S.C. Section 1734 solely to indicate this fact.

Requests for reprints: Jennifer K. Richer, Department of Pathology, University of Colorado Denver, Mail Stop 8104, P.O. Box 6511, Aurora, CO 80045. Phone: 303-724-3735; Fax: 303-724-3712. E-mail: Jennifer.Richer@ucdenver.edu

Copyright © 2009 American Association for Cancer Research.

doi:10.1158/1535-7163.MCT-08-1046

restoring E-cadherin. We find that reinstatement of miR-200c leads to a dramatic decrease in cell migration and invasion and an up to 85% increase in sensitivity to microtubule-targeting chemotherapeutic agents. We suspected that, just as miR-200c indirectly maintains E-cadherin expression by directly repressing ZEB1 and ZEB2, it also likely targets other genes involved in polarity, migratory capacity, and chemosensitivity. Consequently, we performed expression profiling to identify additional genes altered by restoration of miR-200c to cancer cells. Indeed, we find that miR-200c inhibits a program of mesenchymal genes, in addition to ZEBs. We show that one such gene, class III β -tubulin (*TUBB3*), a microtubule component normally found only in neuronal cells, is a direct target of miR-200c. Because expression of *TUBB3* is a prevalent mechanism of resistance to microtubule-binding chemotherapeutic agents in many solid tumors, the fact that *TUBB3* is reduced by miR-200c may account for the dramatic effect of restoration of miR-200c expression on sensitivity to this clinically important class of chemotherapeutic agents.

Materials and Methods

Cell Culture

Hec50 cells, which well represent the more aggressive type 2 endometrial cancers (19), were cultured in DMEM with 10% fetal bovine serum (FBS) and 2 mmol/L L-glutamine. AN3CA cells (American Type Culture Collection), derived from a grade 3 endometrioid adenocarcinoma (also an aggressive form of endometrial cancer and thought to represent the characteristics of type 2 endometrial cancers), and Ishikawa cells (representing a low-grade endometrioid adenocarcinoma, or type 1 tumor; ref. 19) were grown in MEM with 5% FBS, nonessential amino acids, and 1 nmol/L insulin. EEC B37 cells are normal endometrial epithelial cells that have been immortalized with hTERT (20) and were maintained in F12 MEM containing 10% FBS, 2 mmol/L L-glutamine, and 160 ng/mL insulin. HIESC are normal endometrial stromal cells transformed with SV40 large T antigen (21) and were grown in RPMI with 10% FBS, penicillin, streptomycin, and sodium pyruvate. MCF-7 and T47D breast cancer cells were grown in DMEM, 10% FBS, and L-glutamine. BT-474 cells were grown as above, with the addition of nonessential amino acids and insulin. MDA-MB-231 and ZR75 cells were grown in medium containing 5% FBS, HEPES, nonessential amino acids, L-glutamine, penicillin, streptomycin, and insulin. BT-549 cells were grown in RPMI supplemented with 10% FBS and insulin. MCF-7, T47D, ZR75, and BT-474 are all relatively well-differentiated breast cancer cell lines that retain estrogen receptors and the epithelial marker E-cadherin. In contrast, MDA-MB-231 and BT-549 cells represent less differentiated breast cancers negative for estrogen receptors and E-cadherin. All of the ovarian cell lines (2008, Hey, SKOV3, OVCA 420, and OVCA 433) were grown in RPMI with 10% FBS. All cells were grown in a 37°C incubator with 5% CO₂. The identity of all the cell lines was confirmed by DNA profiling using the Identifiler Kit from Applied Biosystems.

Immunoblotting

Whole-cell protein extracts were denatured, and 50 μ g were separated on 8% SDS-PAGE gels and transferred onto polyvinylidene difluoride membranes. After blocking in 5% milk in TBS-T, membranes were probed overnight at 4°C. Primary antibodies used include ZEB1 (rabbit polyclonal from Dr. Doug Darling, University of Louisville, Louisville, KY; 1:1,500 dilution), E-cadherin (clone NCH-38 from DAKO; 1 μ g/mL), N-cadherin (clone 13A9 from Upstate; 1:5,000 dilution), vimentin (clone V9 from Sigma; 1:2,000 dilution), *TUBB3* (clone SDL3D10 from Sigma; 1:400 dilution), PSTAIR (rabbit polyclonal from Upstate; 1 μ g/mL), and α -tubulin (clone B-5-1-2 from Sigma; 1:15,000 dilution). After incubation with appropriate secondary antibody, results were detected using Western Lightning Chemiluminescence Reagent Plus (Perkin-Elmer).

Real-time Reverse Transcription-PCR

RNA was harvested from cells using Trizol (Invitrogen). Before generating cDNA, mRNA was treated with DNase 1 (Invitrogen) for 15 min at room temperature. RNA was reverse transcribed into cDNA in a reaction containing reaction buffer, 10 mmol/L DTT, 1 mmol/L deoxynucleotide triphosphates, RNase inhibitor (Promega), random hexamers (250 ng), and 200 units of MULV-RT (ABI). The reaction proceeded at 25°C for 10 min, then at 37°C for 1 h. For normalization, real-time reverse transcription-PCR (RT-PCR) was done on the cDNA using eukaryotic 18S rRNA endogenous control primers and FAM-MGB probe (ABI). TaqMan MicroRNA Reverse Transcription kit was used to generate cDNA for real-time RT-PCR reaction in conjunction with a miR-200c-specific primer and probe (ABI, assay ID 002300). The reverse transcription primer for miR-200c is a hairpin primer that is specific for the mature miRNA and will not bind to the precursor molecules. Reported values are the means and SEs of three or four biological replicates, as indicated. For validation of the microarray data, SYBR Green real-time RT-PCR was done using primers specific for *CHK2* (forward 5'-GCTCTTGGCTGTGCAGATTA-3', reverse 5'-ACGGTTA-TACCCAGCAGTCC-3'), *ARHGDI1* (forward 5'-CTGGGT-CCCTCTTCAACACT-3', reverse 5'-TGTTCTAGGGAC-CACGTTGA-3'), *MAL2* (forward 5'-GCAGCCACTCCT-GAGTGATA-3', reverse 5'-CGTAAAGCCAGACCCA-AACT-3'), *EPHB1* (forward 5'-GTGAGATGGACAGCTC-CAGA-3', reverse 5'-ACGATCCCATAGCTCCAAAC-3'), *LEPR* (forward 5'-ATTGGAGCAATCCAGCCTAC-3', reverse 5'-CAGGGGCTTCCAAAGTAAAG-3'), *ST6GAL-NAC5* (forward 5'-TGAGCTCTTCAAGCAGGAGA-3', reverse 5'-CATTGTAAACCAGCCAGTGC-3'), and *TUBB3* (forward 5'-CGAAGCCAGCAGTGTCTAAA-3', reverse 5'-GGAGGACGAGGCCATAAATA-3'). To avoid the possibility of amplification artifacts, the PCR products for all SYBR Green primer pairs were verified by gel electrophoresis to be single products.

The relative mRNA or miRNA levels were calculated using the comparative C_t method ($\Delta\Delta C_t$). Briefly, the C_t (cycle threshold) values for the rRNA or actin were subtracted from C_t values of the target gene to achieve the

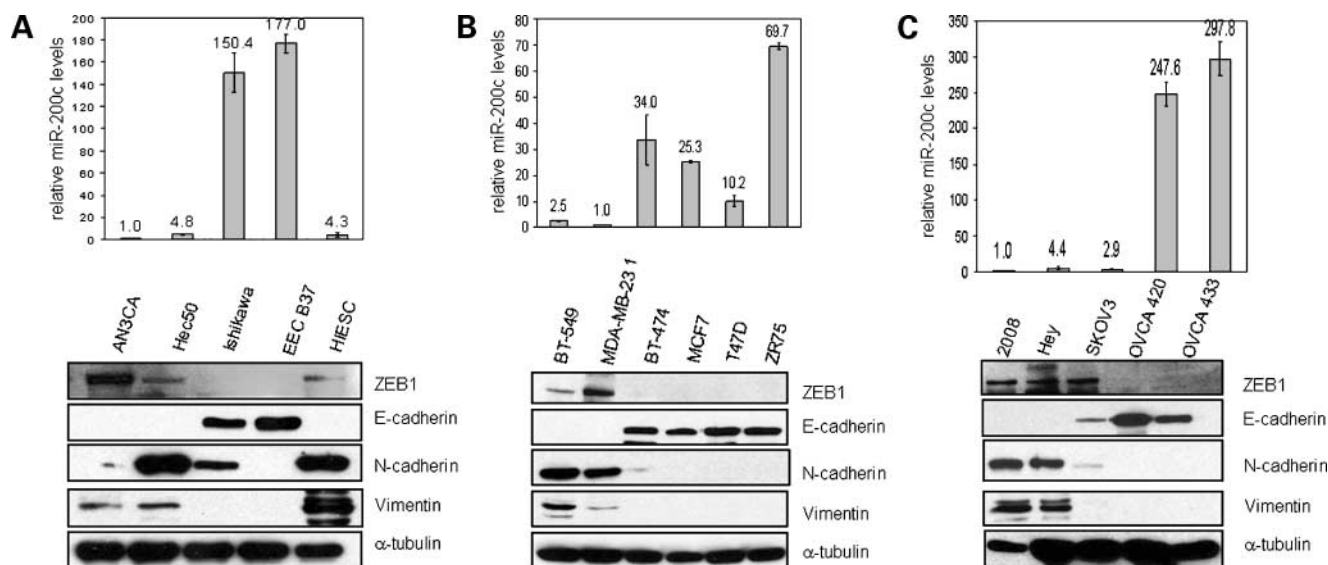


Figure 1. miR-200c and ZEB1 are inversely correlated in endometrial, breast, and ovarian cancer cells. **A**, RNA and protein were harvested from endometrial cancer cell lines—AN3CA and Hec50 (high-grade, representing type 2 endometrial cancers), and Ishikawa (representing type 1 endometrial cancer), EEC B37 (hTERT transformed normal endometrial epithelial cells), and HIESC (SV40 transformed normal endometrial stromal cells). RNA was assayed for miR-200c by real-time PCR (*top*). Immunoblots of whole-cell protein extracts were probed for ZEB1, E-cadherin, N-cadherin, vimentin, and α -tubulin as a loading control (*bottom*). **B**, RNA and protein were harvested from aggressive breast cancer cell lines (BT-549 and MDA 231) as well as the more differentiated cell lines (BT-474, MCF7, T47D, and ZR75) for detection of miR-200c and immunoblot analysis of epithelial and mesenchymal markers. **C**, ovarian cell lines (2008, Hey, SKOV3, OVCA 420, and OVCA 433) were harvested and assayed as above. Each graph is representative of three independent experiments. For real-time RT-PCR, each column represents the mean of quadruplicate samples and bars represent SE. miR-200c levels are normalized to rRNA and are relative to AN3CA, MDA-MB-231, or 2008 cells, respectively.

ΔC_t value. The $2^{-\Delta C_t}$ was calculated for each sample and then each of the values was then divided by a control sample to achieve the relative mRNA or miRNA levels ($\Delta \Delta C_t$).

Transfection, Migration, and Invasion Assays

Lipofectamine 2000 (Invitrogen) was incubated with pre-200c (miRNA mimic) or scrambled negative control (Ambion) at a concentration of 60 nmol/L incubated in serum-free DMEM for 20 min before addition to Hec50 cells. Cells were incubated at 37°C for 4 h before replacement of FBS to 10%. Protein and RNA were harvested 48 h after transfection. For wound healing assay, 24 h after transfection, cells were trypsinized and plated into six-well dishes in triplicate at high density. The next day, a wound was made through the cells using a p200 tip. Pictures were taken immediately and then 4, 8, 12, and 24 h later. For migration and invasion assays, 36 h after transfection, cells were serum starved for 12 h before performing the assay. BD BioCoat Control Insert Chambers 24-well plate with 8- μ m pore size and BD BioCoat Matrigel Invasion Chambers were used for migration and invasion assays, respectively. After starvation, cells were trypsinized and 2.5×10^4 cells were plated in 0.5 mL MEM with 0.5% FBS in the upper chamber. In the lower chamber, 0.8 mL of 50% conditioned medium from Hec50 cells plus 50% DMEM with 10% FBS and L-glutamine was used as an attractant. Cells were incubated for 48 h at 37°C. Migrating or invading cells on the lower surface of the membranes were stained with Diff-Quik stain (Fisher) and counted manually using ImagePro Plus software (Mediacybernetics, Inc.).

Fluorescent Immunocytochemistry

Cells were grown on glass coverslips, rinsed with PBS, and fixed with 10% neutral buffered formalin for 5 min, followed by 50% ethanol for 4 min. Coverslips were rinsed again with PBS and stored dry at -20°C . Before staining, coverslips were thawed at room temperature and rinsed with TBS-T (0.05%). ZEB1 antibody was used at 1:1,000 dilution and E-cadherin at 1:50. Staining was done as described previously (1).

Cell Death ELISAs

Hec50 cells were transfected as described above. Twenty-four hours after transfection, cells were treated with 0, 5, 10, 15, 20, or 25 nmol/L of paclitaxel (Sigma) or with 0, 20, 30, 40, or 50 μ mol/L cisplatin [*cis*-diamminedichlorido-platinum(II); Sigma]. In separate experiments, Hec50 (endometrial cancer), MDA-MB-231 (breast cancer), and Hey (ovarian cancer) cell lines were treated with tumor necrosis factor-related apoptosis-inducing ligand (TRAIL; R&D Systems) at 50 ng/mL, FasL (Axxora Life Science, Inc.) at 1 μ g/mL, doxorubicin (Calbiochem) at 6 μ g/mL, mitomycin C (Sigma) at 100 nmol/L, vincristine (Sigma) at 100 nmol/L, or epothilone B (Sigma) at 100 nmol/L. Twenty-four hours after treatment, the Cell Death ELISA (Roche), which recognizes mononucleosomes and oligonucleosomes in the cytoplasm of dying cells, was done as per manufacturer's instructions.

Statistical Analysis

For the real-time PCR, cell death ELISA, and luciferase assays, a Student's paired *t* test was done to determine

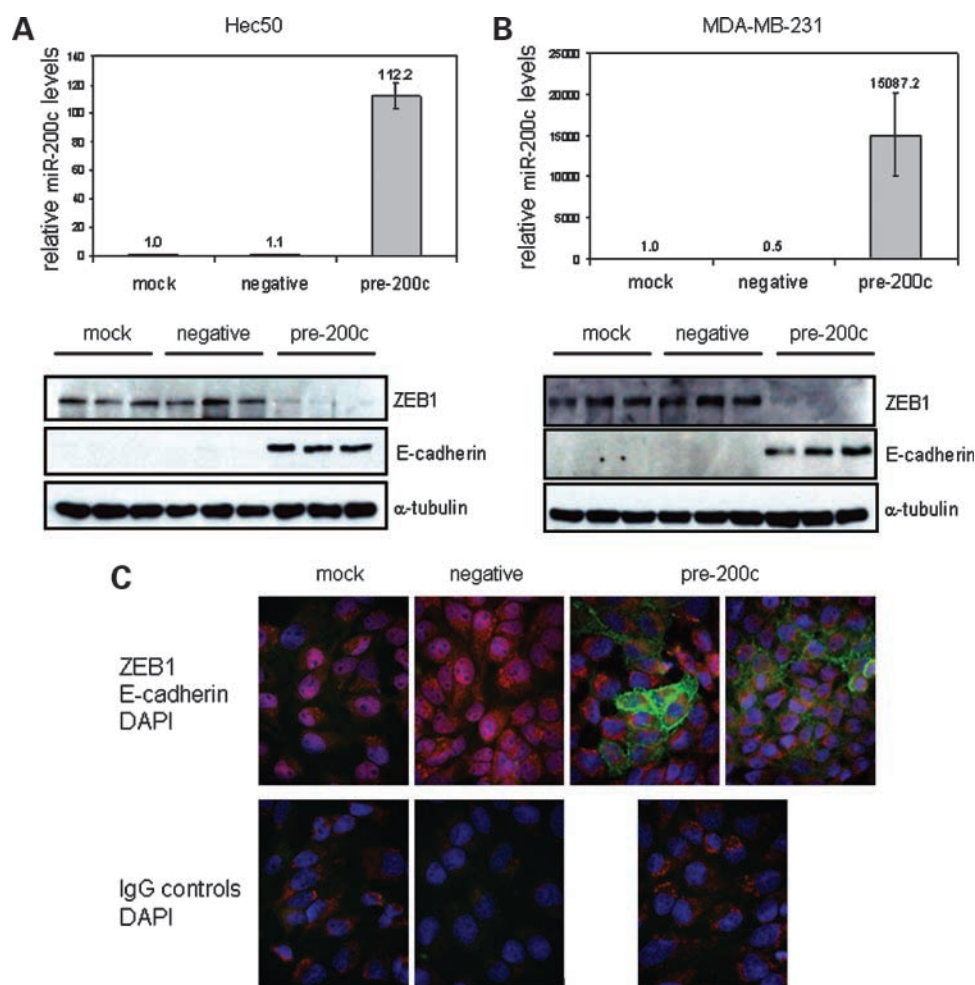


Figure 2. Addition of exogenous miR-200c results in repression of ZEB1 and restoration of E-cadherin protein. Hec50 endometrial cancer cells (**A**) and MDA-MB-231 breast cancer cells (**B**) were treated with transfection reagent only (*mock*), scrambled negative control mimic (*negative*), or miR-200c mimic (*pre-200c*). After 48 h, RNA was harvested and miR-200c levels were determined by real-time PCR (*top*). Columns, mean of quadruplicate samples; bars, SE. The miR-200c levels are normalized to rRNA and are relative to mock transfection levels. Western blots of protein from the three experimental groups (mock, negative, or miR-200c treated) were probed for ZEB1, E-cadherin, and α -tubulin as a loading control. Three replicates per treatment group are shown. For both real-time RT-PCR and Western blots, results are representative of one of three independent experiments. **C**, Hec50 cells grown on coverslips were treated as above and fluorescent immunocytochemistry results using antibodies recognizing ZEB1 (*red*), E-cadherin (*green*), and 4',6-diamidino-2-phenylindole (DAPI; *blue*) are shown merged. *Bottom*, relevant IgG-negative controls. Magnification, $\times 1,000$.

statistical significance (Microsoft Excel). Values were considered to be statistically significant if $P \leq 0.05$.

Microarray Analysis

To confirm the integrity of triplicate RNA samples, RNA-nano chips were run on a Bioanalyzer (Agilent). The cDNA was generated and processed according to the GeneChip Expression Analysis Technical Manual (Affymetrix). Labeled complementary RNA was made using the GeneChip_IVT Labeling Kit (Affymetrix), fragmented, and hybridized to HGU133 Plus 2.0 Affymetrix oligonucleotide microarray chips, which contain $>54,000$ probe sets. GeneSpring GX 9.0 (Agilent) software was used for analysis and clustering of array data. Data were filtered using a 1.5-fold change cutoff and a P value of 0.05 (ANOVA, with Benjamini Hochberg FDR multiple testing correction). Ingenuity Pathway Analysis software (Ingenuity Systems) was used to determine which pathways are highly represented among the genes that change in response to miR-200c.

Luciferase Assays

A 262-bp section of the 3' untranslated region (UTR) of *TUBB3* containing the putative binding site for miR-200c (predicted from the TargetScan database) was amplified by

PCR from HeLa genomic DNA using the following primers: *TUBB3* F, 5'-CCACTAGTCGACGAGGAGGAGT-3', and *TUBB3* R, 5'-CTCAAGCTTGCTGGAGCTGCA-3'. The fragment was cloned into the 3'-UTR of a firefly luciferase reporter vector (pMIR-REPORT, Ambion) using *Hind*III and *Spe*I. To generate the *TUBB3* 3'-UTR containing a mutation in the miR-200c binding site, the following primers were used (mutation in bold): *TUBB3*mutF, 5'-CCTGCATCTTT-TATGGCCT-CG-3', and *TUBB3*mutR, 5'-CATAAAAGATG-CAGGAGGGCGGCAAGG-3'. Two PCR products were generated using the primer pairs of *TUBB3*F with *TUBB3*-mutR and *TUBB3*R with *TUBB3*mutF. These two PCR products were annealed and used as template for a final PCR reaction generated using the *TUBB3*F and *TUBB3*R primers. This generated the final product containing the mutated site, which was cloned into pMIR-Report. Hec50 cells (15,000 per well) in a 96-well plate were transfected with the negative control or pre-200c as described above. After 24 h, the firefly reporter plasmid (0.196 μ g) and a renilla luciferase normalization plasmid pRL-SV40 (0.004 μ g) were introduced using Lipofectamine 2000. Cells were harvested 48 h later for analysis using the Dual Luciferase Reporter assay system (Promega).

Results

Low MiR-200c Expression Strongly Correlates with Lack of E-cadherin Expression and Gain of Mesenchymal Markers Including ZEB1

We sought to determine if there is a negative correlation between miR-200c and ZEB1 in a panel of endometrial cancer cell lines. Hec50 and AN3CA cells, derived from a serous papillary uterine cancer and a grade 3 endometrioid adenocarcinoma respectively, are highly aggressive and are good models of the behavior of type 2 endometrial cancers (19). In contrast, Ishikawa cells are derived from a well-differentiated, less aggressive type 1 endometrial cancer. EEC B37, a cell line derived from normal endometrial epithelial cells (20), and HIESC, derived from normal endometrial stromal cells (21), were also examined. The miR-200c levels were extremely low in the poorly differentiated type 2 endometrial cell lines and the stromal cell line (Fig. 1A). In comparison, the normal endometrial epithelial cell line and the Ishikawa cells had >150-fold higher miR-200c levels. These results suggest that loss of miR-200c expression is associated with poorly differentiated endometrial carcinoma. Stromal cells also express low levels of miR-200c, consistent with our observa-

tion that ZEB1 is expressed in normal endometrial stroma (1, 2). Immunoblot results reveal that ZEB1 protein is present in the type 2 cell lines (AN3CA and Hec50) as well as in normal stromal cells, but normal epithelial cells and the well-differentiated Ishikawa cancer cells lack ZEB1. Because ZEB1 is a potent repressor of E-cadherin, E-cadherin protein is present only in the normal epithelial cells and Ishikawa cells, which express miR-200c robustly and lack ZEB1. More aggressive endometrial cancers often undergo EMT and begin to express stromal markers (1, 2). The normal stromal cells (HIESC) and the more aggressive cancer cell lines, Hec50 and AN3CA, all express vimentin. Only Hec50 and HIESC cells express N-cadherin. In contrast, neither the normal epithelial cells nor the Ishikawa cells express vimentin and the normal cells lack expression of N-cadherin. We observe a similar negative correlation between miR-200c and ZEB1 expression and a positive correlation between miR-200c and E-cadherin in a panel of breast (Fig. 1B) and ovarian (Fig. 1C) cancer cells.

Restoration of MiR-200c Restores E-cadherin Expression and Reduces Migration and Invasion

To determine if miR-200c controls ZEB1 expression in endometrial cancer cells, we used a commercially available

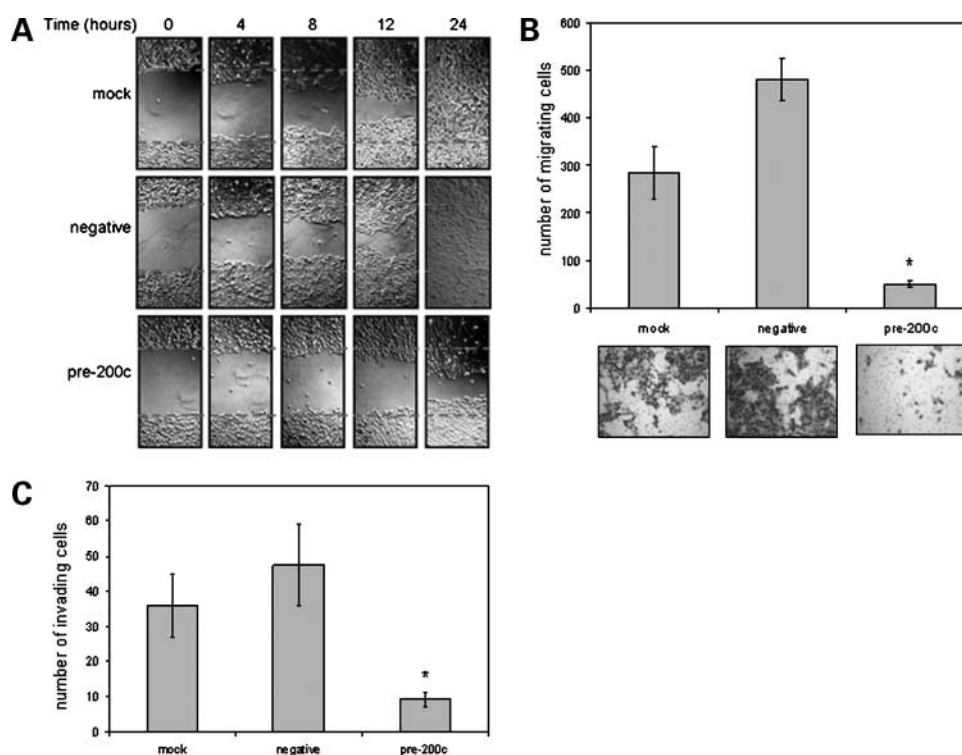


Figure 3. Restoration of miR-200c expression in Hec50 decreases migration and invasion. **A**, Hec50 cells were treated with transfection reagent only, a scramble negative control, or miR-200c mimic. After 48 h, wounds were inflicted and pictures taken at 0, 4, 8, 12, and 24 h after wounding. Lines indicate width of the wound at time zero. Pictures shown are from one experiment representative of three separate experiments (not shown). **B**, mock-, negative-, or miR-200c-transfected cells were subjected to a transwell migration assay. After 48 h, cells on the bottom side of the membrane were stained and mounted onto slides and the mean number of cells in four fields of vision on a cross-hatch was counted with error bars representing SE of four replicates. *, statistically significant difference between the numbers of cells migrating in the pre-200c, compared with either mock-transfected cells or negative control-treated cells [$P = 2.8 \times 10^{-4}$ and $P = 6.0 \times 10^{-8}$, respectively (Student's *t* test)]. Representative images ($\times 100$ magnification) of stained filters are shown. **C**, the number of cells able to invade through Matrigel-coated Boyden chambers was also determined for each group. Columns, mean number of cells from four replicates; bars, SE. *, statistically significant difference between the pre-200c-treated group, compared with either mock-transfected cells or negative control-treated cells [$P = 0.0039$ and $P = 0.0020$, respectively (Student's *t* test)].

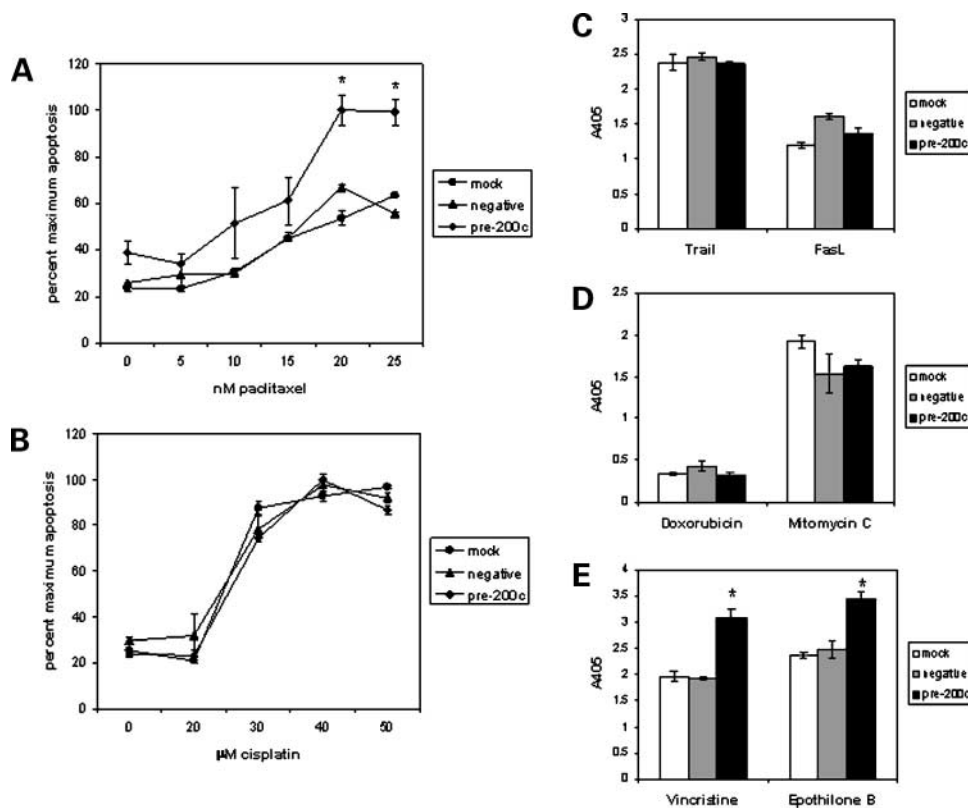


Figure 4. MiR-200c alters cell death in response to microtubule-targeting chemotherapeutic agents specifically. Hec50 cells were treated with transfection reagent only (*mock*), scrambled negative control (*negative*), or miR-200c mimic (*pre-200c*). Twenty-four hours after transfection, cells were treated with 0, 5, 10, 15, 20, or 25 nmol/L of paclitaxel (**A**) or with 0, 20, 30, 40, or 50 μmol/L of cisplatin (**B**) and, 24 h after drug treatment apoptosis, were assayed using a Cell Death ELISA. Points, percent maximum apoptosis; bars, SE of triplicate samples. This experiment was done twice and representative experiments for each drug are shown. *, $P < 0.05$, between pre-200c-treated cells and mock or negative controls (Student's t test). Hec50 cells treated with pre-200c or negative controls were treated with agents that cause apoptosis via cell surface receptors (TRAIL, 50 ng/mL or FasL, 125 ng/mL; **C**), DNA damage (doxorubicin, 1 μg/mL or mitomycin C, 6 μg/mL; **D**), or microtubule poisons (vincristine, 100 nmol/L or etoposide, 100 nmol/L; **E**), and Cell Death ELISAs were done. Columns, mean of five replicates; bars, SE. The experiment was repeated on three separate occasions with the same result, and a representative experiment is shown. *, $P < 0.05$, between pre-200c and both the mock and negative controls (Student's t test).

miR-200c mimic (*pre-200c*) to restore miR-200c to Hec50 cells. A time course measuring miR-200c following transfection with the mimic showed maximum levels of expression achieved by 24 hours, gradually decreasing over 6 days, while still remaining above control level (data not shown). At 48 hours after transfection, we achieved a 112-fold expression of miR-200c over mock-transfected and scrambled control-containing cells (Fig. 2A, top). Importantly, at the concentration used for transient transfections, the levels of miR-200c achieved are comparable to the endogenous miR-200c levels found in the well-differentiated Ishikawa cells (Fig. 1A). Increasing miR-200c causes inhibition of ZEB1 expression and, importantly, a complete restoration of E-cadherin protein expression (Fig. 2A, bottom). To ensure that these effects were not cell type specific, we also performed a transient transfection of pre-200c into MDA-MB-231 cells, an aggressive breast cancer cell line (Fig. 2B). As seen in Fig. 2A and B (bottom), restoration of miR-200c to the MDA-MB-231 cells also causes an almost complete repression of ZEB1 levels, resulting in a dramatic appearance of E-cadherin expression. Dual fluorescence immunocyto-

chemistry done on coverslips from the Hec50 transfection experiment show that whereas no E-cadherin (green) is observed in the negative control and mock-transfected cells, there is a low level of E-cadherin expression in the majority of the pre-200c-treated cells and very high expression in some areas (Fig. 2C), as would be expected in a transient transfection. There is a decrease in nuclear ZEB1 staining (red, or pink when overlaid with 4',6-diamidino-2-phenylindole) in the pre-200c-treated cells. Some apparent ZEB1 staining occurs in the cytoplasm in all treatment groups; however, this is likely nonspecific because it is also observed in the isotype antibody control.

To determine if introducing miR-200c renders Hec50 cells less migratory, a wound healing assay was done on the pre-200c-treated cells as well as the negative controls. Figure 3A shows that Hec50 cells treated with pre-200c are distinctively less migratory than the negative control and mock-transfected cells. Furthermore, a transwell migration assay showed a similar loss of migratory capacity (Fig. 3B). Decreases of 82% and 89% in the number of migrating cells were observed in the pre-200c-treated cells compared with

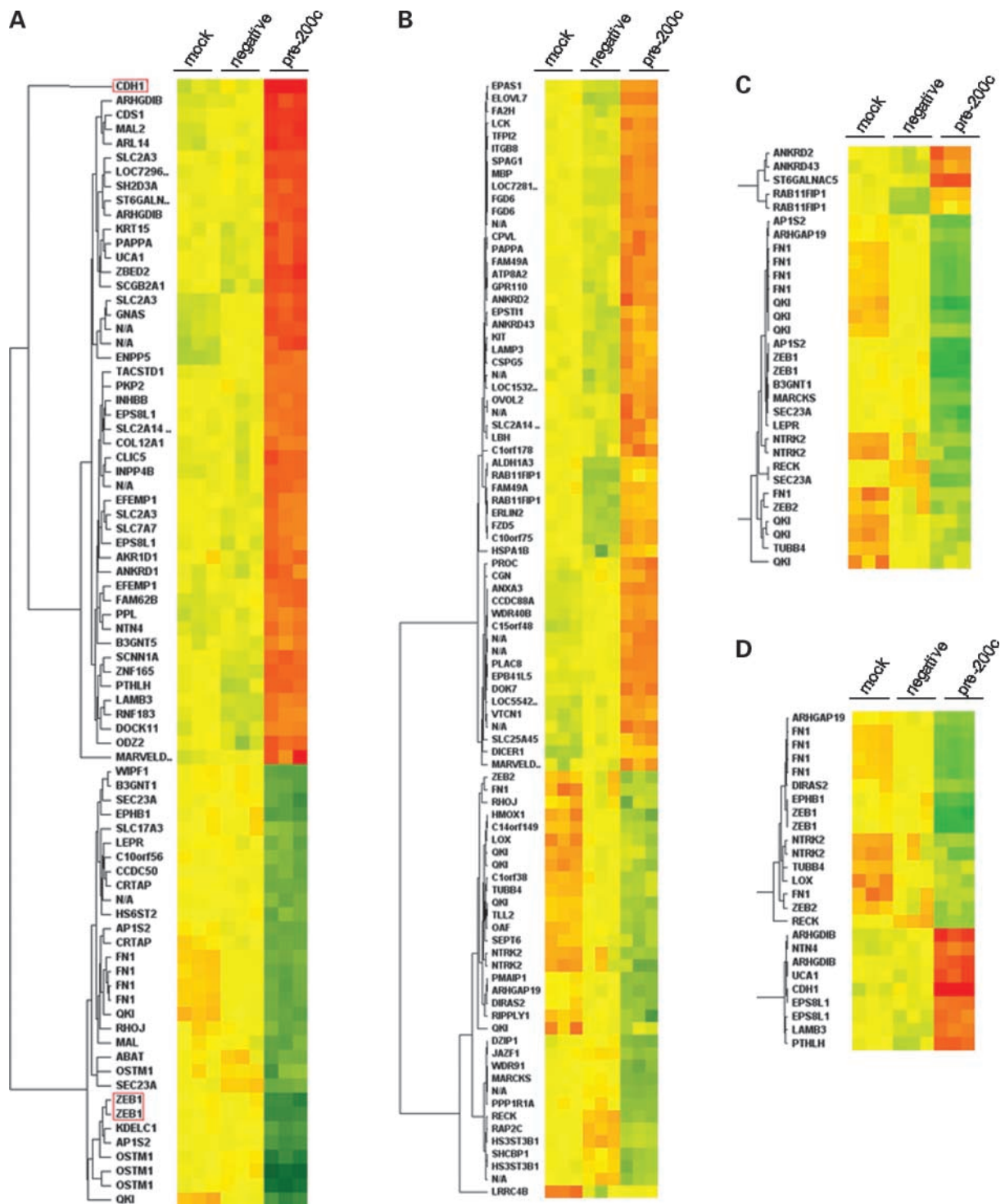


Figure 5. Heatmap of genes significantly affected by restoration of miR-200c levels in Hec50 cells as determined by expression profiling. Hec50 cells were treated in triplicate with mock, negative control, or pre-200c transfection, and gene expression analysis was done on Affymetrix HGU133 Plus 2.0 oligonucleotide cDNA expression array chips. **A**, genes with a statistically significant (ANOVA) ≥ 1.5 -fold up-regulation (red) or down-regulation (green) in the pre-200c-treated cells versus both the negative control and the mock-transfected cells are shown in a heatmap. Expected alterations in *E-cadherin* (*CDH1*) and *ZEB1* are highlighted. **B**, genes ≥ 1.5 -fold up-regulated or down-regulated in the pre-200c-treated cells versus either negative control are shown in a separate heatmap. **C**, a heatmap of genes from **A** or **B** that are bioinformatically predicted to be targets of miR-200c. **D**, genes differentially regulated by miR-200c implicated in cell migration as determined by Ingenuity Pathway Analysis. Note that each gene was normalized to its average expression over the nine chips, such that the intensities center around 1 and are presented on a scale of -2 to $+2$ and are thus not indicative of relative fold changes. Fold changes and *P* values for these genes are listed in Supplementary Table S1.¹

the mock-transfected or negative control-treated cells, respectively. In addition, 81% fewer pre-200c-treated cells were able to invade through Matrigel in a transwell invasion assay as compared with negative control-treated cells (Fig. 3C). MiR-200c did not affect the amount of proliferation of the cells as measured with 3-(4,5-dimethylthiazol-2-yl)-2,5-diphenyltetrazolium bromide and Hoechst dye assays (data not shown).

Restoration of MiR-200c Enhances Chemosensitivity to Microtubule-Directed Agents

To determine if restoration of miR-200c and the resulting reestablishment of epithelial characteristics would affect chemosensitivity, paclitaxel- and cisplatin-induced apoptosis were measured in cells treated with pre-200c versus controls. A significant increase in chemosensitivity to paclitaxel (Fig. 4A), but not cisplatin (Fig. 4B), was detected in Hec50 cells transfected with miR-200c. The chemosensitivity to 25 nmol/L paclitaxel was increased by 37% and 45% in the cells treated with pre-200c versus the mock and negative controls, respectively. Because paclitaxel and cisplatin have different modes of action, we performed further cell death ELISAs using agents that induce apoptosis via different mechanisms. FasL and TRAIL induce death through tumor necrosis factor-related cell surface receptors in a caspase-8-dependent manner. No increase in chemosensitivity to either TRAIL or

FasL was observed with pre-200c treatment (Fig. 4C). Doxorubicin and mitomycin C, like cisplatin, cause DNA damage that results in apoptosis, and neither agent caused an increase in chemosensitivity in conjunction with pre-200c treatment (Fig. 4D). Epothilone B and vincristine both cause apoptosis by stabilization of microtubules in a mechanism similar to that of paclitaxel. As observed with paclitaxel, pre-200c treatment causes substantial and statistically significant increase in chemosensitivity to these two additional microtubule poisons (Fig. 4E).

Identification of Direct and Downstream Targets of MiR-200c

Whereas it has been previously shown that miR-200c regulates ZEB1 and ZEB2, many other putative miR-200c targets are predicted by bioinformatics based on complementarity, but remained to be validated. To identify miR-200c direct targets or genes downstream of such targets that might be responsible for the reduction in invasiveness and increased sensitivity to microtubule-targeting agents, expression profiling was done on Hec50 cells treated with pre-200c as compared with mock- or scrambled control-transfected cells. Our profiling study identified a cluster of genes significantly differentially regulated by miR-200c as compared with both controls (mock- and scrambled nontargeting miRNA-transfected cells; Fig. 5A). Additional

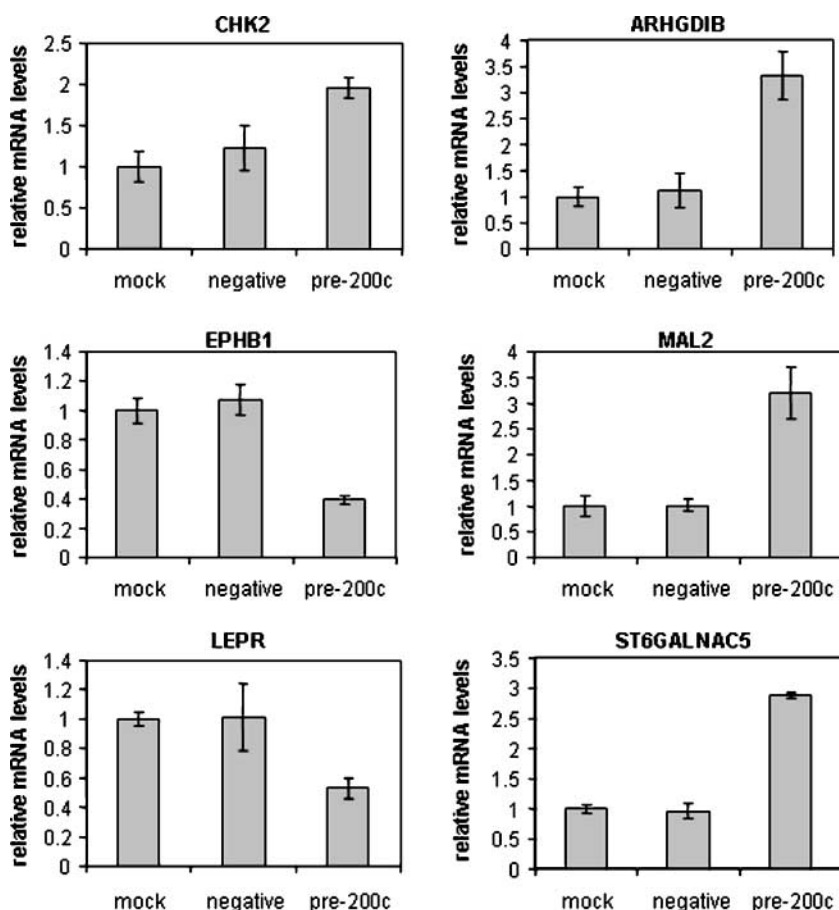


Figure 6. Select genes altered by restoration of miR-200c are validated by RT-PCR. SYBR Green real-time RT-PCR was done on Hec50 cells treated with transfection reagent only (*mock*), 60 nmol/L of a scramble negative control (*negative*), or 60 nmol/L of the miR-200c mimic (*pre-200c*) using primers specific for *CHK2*, *ARHGDI1*, *EPHB1*, *MAL2*, *LEPR*, and *ST6GALNAC5*. Bars, SE of three replicates.

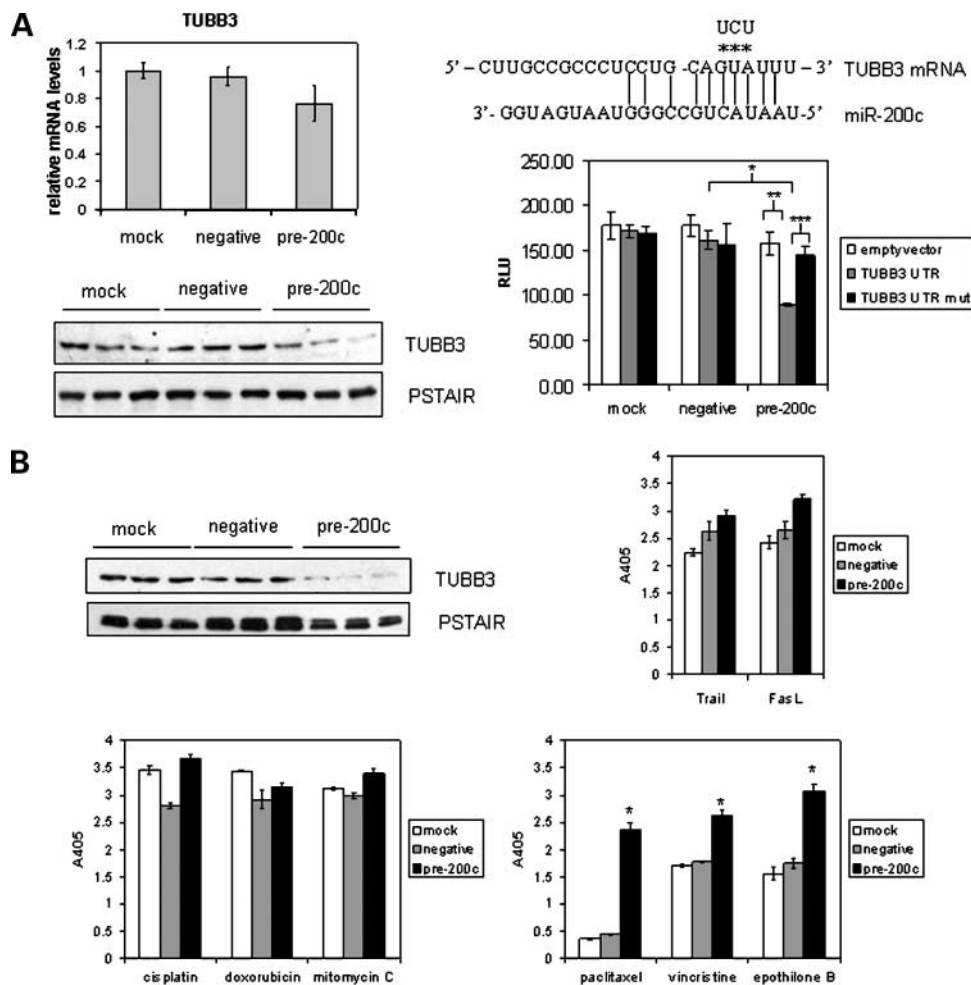


Figure 7. A site in the *TUBB3* 3'-UTR is a direct target of miR-200c, and a decrease in TUBB3 protein corresponds with an increase in cell death in response to microtubule-targeting agents. **A**, SYBR Green real-time RT-PCR using primers specific for *TUBB3* was done on RNA from Hec50 cells treated with miR-200c mimic (*pre-200c*), negative scrambled control (*negative*), or mock-transfected (*mock*) control (*top left*). A corresponding Western blot consisting of protein from the same cells was probed for TUBB3 (*bottom left*) and PSTAIR (used as a loading control). A fragment of the *TUBB3* 3'-UTR (located 117–379 bp after the stop codon) containing the putative miR-200c binding site, or the same fragment with the indicated base pairs that bind to the miR-200c seed sequence mutated, was cloned into the luciferase reporter vector pMIR-REPORT. These constructs, empty pMIR-REPORT vector, vector containing wild-type *TUBB3* 3'-UTR, or mutated *TUBB3* 3'-UTR (*TUBB3* UTR mut), were transfected into Hec50 cells following negative control, *pre-200c*, or mock transfection. A dual reporter luciferase assay was done, and relative luciferase units (RLU) were calculated as firefly luciferase values divided by renilla values. *Columns*, mean of five replicate samples; *bars*, SE. *, $P = 0.041$, statistically significant difference in the amount of luciferase detected when the wild-type *TUBB3* UTR is in the presence of *pre-200c* versus negative control. **, $P = 0.006$, difference in the amount of luciferase in the presence of *pre-200c* and either the empty vector or wild-type *TUBB3* 3'-UTR-containing reporter. ***, $P = 0.003$, difference between the amounts of luciferase measured when it is targeted by wild-type versus mutated *TUBB3* 3'-UTR. **B**, an aggressive ovarian cancer cell line, Hey, was treated with *pre-200c*, a negative control, or mock transfection. *Top left*, Western blot for TUBB3 with PSTAIR as a loading control. A Cell Death ELISA was done on the mock-, negative control-, or *pre-200c*-transfected Hey cells treated with various chemotherapeutic agents. *Top right*, Trail and FasL; *bottom left*, cisplatin, doxorubicin, and mitomycin C; *bottom right*, paclitaxel, vincristine, and epothilone B. *Asterisks*, statistically significant differences (as determined by Student's *t* tests) between the *pre-200c*-treated cells versus negative- and mock-transfected controls individually ($P = 5.8 \times 10^{-5}$ and $P = 7.9 \times 10^{-5}$, *pre-200c* versus mock and negative control, respectively, in the paclitaxel-treated group; $P = 0.0005$ and $P = 0.0009$, *pre-200c* versus mock and negative control, respectively, in the vincristine-treated group; and $P = 1.3 \times 10^{-5}$ and $P = 2.3 \times 10^{-5}$, *pre-200c* versus mock and negative control, respectively, in the epothilone B-treated group).

genes significantly different in the *pre-200c*- versus mock-transfected or negative control-treated cells, but not both, are shown in Fig. 5B. As expected, on addition of miR-200c, *E-cadherin* (*CDH1*) was up-regulated (on average, 10.8-fold) and *ZEB1* was down-regulated (by 3.1-fold). A complete list of genes significantly affected by miR-200c with fold changes and *P* values is provided

in Supplementary Table S1.¹ Further validation of the microarray results is the fact that 18 putative direct targets of miR-200c, as predicted by bioinformatics using Sanger miRBase, TargetScan, and PicTar databases (including

¹ Supplementary material for this article is available at Molecular Cancer Therapeutics Online (<http://mct.aacrjournals.org/>).

ZEB1 and *ZEB2*), are differentially regulated in the miR-200c-treated cells (Fig. 5C) as compared with controls. The vast majority (14 of 18) of the direct targets are down-regulated by miR-200c restoration. Many of the genes identified are not predicted miR-200c targets, but are likely downstream of direct targets (as is the case with E-cadherin, being downstream of the direct target, *ZEB1*). Interestingly, a significant number of genes affected by pre-200c treatment were recognized by Ingenuity Pathway Software as belonging to a network of genes involved in cellular migration, and these genes are shown in the cluster depicted in Fig. 5D.

To validate the array data, we performed real-time RT-PCR on *CHK2*, *ARHGDI1*, *EPHB1*, *MAL2*, *LEPR*, and *ST6GALNAC5* (Fig. 6A) on independent biological samples. These genes represent both predicted direct targets of miR-200c (*LEPR*, *ST6GALNAC5*) as well as presumed downstream targets (*CHK2*, *ARHGDI1*, *EPHB1*, and *MAL2*). We have also confirmed by RT-PCR that *TUBB3* is modestly decreased at the RNA level; however, we observe a more dramatic decrease in *TUBB3* protein, indicating that miR-200c may also affect translation of *TUBB3* (Fig. 7A, left). To test whether *TUBB3* is a direct target of miR-200c, we cloned the predicted target sequence within the *TUBB3* gene downstream of luciferase in a reporter vector. Figure 7A (right) shows that the amount of luciferase is only significantly decreased by the presence of the *TUBB3* 3'-UTR target sequence when miR-200c mimic is transfected into Hec50 cells, and not in the presence of negative control mimic or the mock-transfected cells. In addition, when the target region of the *TUBB3* 3'-UTR was mutated at 3 bp that bind the seed sequence of miR-200c (see asterisks in Fig. 7A, right), luciferase is no longer reduced, indicating that the miR-200c binding site has been rendered nonfunctional. Furthermore, in the aggressive ovarian cancer cell line Hey, *TUBB3* protein levels are even more dramatically reduced by miR-200c (Fig. 7B, left) than they are in the Hec50 cells. To assay whether a more pronounced decrease in *TUBB3* corresponds with an even greater chemosensitivity to microtubule-targeting agents in the Hey cells, we again performed a cell death ELISA with the panel of chemotherapeutic agents. Similar to the Hec50s, there was no substantial increase in chemosensitivity to agents that cause apoptosis through cell surface receptors or via DNA damage; however, there was a dramatic statistically significant increase in cell death in response to microtubule-targeting agents. The most dramatic increase in response was observed with paclitaxel, in which there is an 82% to 85% increase in chemosensitivity when miR-200c is restored to the cells (Fig. 7B, bottom right). There was also a 33% to 35% increase in chemosensitivity to vincristine in the pre-200c-treated cells and a 43% to 50% increase in response to epothilone B. Interestingly, MDA-MB-231 cells have been reported to be resistant to Taxol by a different method (a mutation in class I β -tubulin; ref. 22), and we observe that miR-200c does not restore chemosensitivity to microtubule-targeting agents in this cell line (data not shown).

Discussion

In this report, we examine the effect of restoring miR-200c expression to poorly differentiated, aggressive endometrial, breast, and ovarian cancer cells. Several recent reports have shown the importance of miR-200c, as well as other miR-200 family members, in the regulation of *ZEB1* and *ZEB2*. Because miRNAs commonly function by binding the 3'-UTRs of genes, the conservation of the target sequences in *ZEB1* and *ZEB2* emphasizes the importance of miR-200-mediated regulation of these genes. MiR-200c maintains "epithelialness" by suppressing *ZEB1* and *ZEB2*. We show that when we put miR-200c back into aggressive endometrial, breast, and ovarian cancer cells that have lost it (restoring it to levels found in normal epithelial cells), we observe dramatic effects on phenotype and behavior. Restoration of miR-200c causes a nearly complete inhibition of *ZEB1* expression and, importantly, a very prominent restoration of E-cadherin protein expression. Others have shown that due to their high degree of sequence homology, other miR-200 family members (miR-141 on the same chromosome, 12p13.31, and miR-200b, miR-200a, and miR-429 on chromosome 1p36.33) have overlapping functions. However, we show that restoration of miR-200c alone is sufficient to suppress *ZEB1* expression, restore E-cadherin, reduce invasive capacity, and restore chemosensitivity to microtubule-targeting agents.

Although *ZEB1* does repress numerous genes involved in polarity (6, 7), we predicted that such a dramatic reversal of phenotype, invasiveness, and chemosensitivity achieved by restoration of miR-200c could not be solely explained by its ability to target *ZEB1* and *ZEB2*. We suspected that just as miR-200c indirectly maintains E-cadherin expression by directly abolishing *ZEB1* (a potent E-cadherin repressor), it also likely both directly and indirectly affects other genes involved in polarity, migratory/invasive capacity, and chemosensitivity. Consequently, we performed expression profiling to identify additional genes statistically significantly affected by restoration of miR-200c in Hec50 endometrial cancer cells.

Whereas it is possible that some direct targets of miR-200c might be missed on a cDNA expression array because miRNAs can affect translation of a target mRNA without causing a change in transcript levels, microarray expression profiling remains a valid method of identifying global gene changes induced by restoration of miR-200c. Indeed, significant alterations in 16 genes (in addition to *ZEB1* and *ZEB2*) predicted by bioinformatics to be direct targets of miR-200c were observed with reintroduction of miR-200c to Hec50 endometrial cancer cells. The majority of the predicted target genes (14 of 18) were down-regulated by miR-200c in our study. Only four (*ANKRD1*, *ANKRD43*, *ST6GALNAC5*, and *RAB11FIP1*) were up-regulated. Although most miRNA targets are down-regulated, there is some evidence that miRNAs can target genes for up-regulation by at least two different mechanisms (23, 24). Some of the interesting predicted direct targets significantly down-regulated by miR-200c in our study include other mesenchymal markers, such as fibronectin 1 (*FN1*), which, like *ZEB1*, is a marker of EMT, and leptin receptor (*LEPR*), which is overexpressed in breast

cancers with poor prognosis and has been implicated in mammary tumorigenesis (25–27). NTRK2 (neurotrophic tyrosine kinase; also known as TrkB) acts as a potent suppressor of anoikis (detachment-induced apoptosis) and is associated with the acquisition of an aggressive tumorigenic and metastatic phenotype *in vivo* (28). QKI, an RNA binding protein, is involved in myelination and binds to mRNAs encoding oncogenes, suggesting a role for QKI in cancer (29, 30).

Like E-cadherin, some of the other genes identified in our screen are known to be repressed by ZEB1; for instance, *MAL2*, *MARVELD2*, *PKP3*, *PPL*, and *TACSTD1* have all previously been identified as ZEB1 targets (6, 7) and were significantly increased by miR-200c in our experiments. *MAL2* is essential for basolateral-to-apical transcytosis and apical trafficking, a defining feature of epithelial cells. Plakophilin 3 (*PKP3*) and periplakin (*PPL*) are components of desmosomes, and *MARVELD2* encodes a tight junction protein. *TACSTD1* (tumor-associated calcium signal transducer 1; also known as EpCAM) encodes a protein expressed on the apical side of epithelial cells.

We also found that restoration of miR-200c increases *ARHGDI3* (Rho GDP-dissociation inhibitor β), an inhibitor of Rho GTPases, which acts as a tumor suppressor and is a negative regulator of migration (reviewed in ref. 31). Thus, in addition to restoring E-cadherin, increasing the tumor suppressor *ARHGDI3* is a potential mechanism whereby miR-200c reduces the migratory/invasive behavior of Hec50 cells. Other genes involved in cytoskeleton reorganization, such as *WIPF1* (WAS/WASL interacting protein), *EPS8L1* (EPS8-like 1), and *CGN* (cingulin), which regulates tight junctions, may also be involved in the ability of miR-200c to modulate cell motility. *EPHB1* (ephrin receptor B1) is a receptor tyrosine kinase involved in cell-cell interactions, angiogenesis, migration, and stem cell polarity (32, 33). In addition, both lysyl oxidase (*LOX*) and fibronectin 1 (*FN1*) are significantly decreased by restoration of miR-200c and they are heavily implicated in metastasis and formation of the premetastatic niche (34–36).

We also show that restoration of miR-200c expression renders Hec50 cells more sensitive to paclitaxel and other microtubule-directed agents such as vincristine and epothilone B, but not to apoptosis-inducing agents that work through death receptors (TRAIL and FasL) or DNA-damaging agents (cisplatin, doxorubicin, or mitomycin C). Intriguingly, our microarray data reveal that the class III β -tubulin (*TUBB3/TUBB4*) gene, a predicted direct target of miR-200c, is significantly down-regulated in the presence of miR-200c. This provided an attractive potential mechanism whereby miR-200c restores chemosensitivity specifically to microtubule-targeting agents because numerous studies have linked overexpression of *TUBB3*, normally only expressed in neuronal cells, with resistance to microtubule-targeting agents in many types of cancers (37–40). We confirmed its down-regulation in the presence of miR-200c at the RNA level and observed an even more dramatic decrease at the protein level in endometrial and ovarian cancer cells, suggesting that miR-200c may regulate *TUBB3* expres-

sion primarily through inhibition of *TUBB3* translation. Furthermore, we show that the predicted miR-200c target site within the *TUBB3* 3'-UTR is indeed a bona fide target of miR-200c, being necessary and sufficient for down-regulation of *TUBB3* by miR-200c. In Hey ovarian cancer cells, we observed an even more pronounced decrease in *TUBB3* protein in response to restoration of miR-200c than observed in Hec50 endometrial cells, and this corresponds with a dramatic 85% increase in chemosensitivity to paclitaxel. The majority of women with advanced ovarian cancer ultimately relapse with drug-resistant disease with an overall 5-year survival of <50%. Several studies have linked expression of *TUBB3* with resistance to microtubule-targeting chemotherapeutics in ovarian cancers (41–44). One of these studies (44) examined the three main mechanisms of paclitaxel resistance (overexpression of *MDR-1* gene, point mutations in α -tubulin and β -tubulin genes, and selective alterations in the expression of β -tubulin isoforms) and found that the only statistically significant difference in the resistant subset of tumors was up-regulation of class III β -tubulin. Thus, we propose that targeting *TUBB3* is a major mechanism whereby miR-200c restores chemosensitivity to microtubule-targeting agents. We propose that in the clinical setting, restoration of miR-200c could render highly aggressive forms of endometrial and ovarian cancers more responsive to microtubule-targeting chemotherapeutic agents and decrease invasive potential as well.

There is increasing evidence that miRNAs play an important role in many aspects of tumorigenesis, and recent reports have implicated the miR-200 family in EMT via direct repression of ZEB1 and ZEB2. Here we extend this developing paradigm by showing that loss of miR-200c is associated with type 2 endometrial carcinomas as well and that restoration of miR-200c to aggressive endometrial cancer cells results in reestablishment of epithelial identity. E-cadherin and other markers of polarity are reexpressed; cells are rendered substantially less invasive and become significantly more sensitive to microtubule-targeting chemotherapeutic agents. We identify additional genes (other than ZEB1 and ZEB2) directly and indirectly targeted by miR-200c, which are likely responsible for restoration of the epithelial state; decrease in migratory capacity; and increased sensitivity to microtubule-targeting chemotherapeutics. We suggest that loss of miR-200c will be predictive of aggressive behavior and resistance to microtubule-targeting agents, and that restoration of miR-200c has potential as a therapeutic strategy for treating highly metastatic, drug-resistant, and thus otherwise relatively untreatable, cancers.

Disclosure of Potential Conflicts of Interest

No potential conflicts of interest were disclosed.

Acknowledgments

We thank Monique Spillman, MD., Ph.D. (Department of Medicine, Division of Endocrinology, University of Colorado Denver, Aurora, Colorado) and Barb Helfrich, M.S. (Medical Oncology, University of Colorado Denver, Aurora, Colorado) at the University of Colorado Denver for providing ovarian cancer cell lines. We acknowledge Christopher Korch, Ph.D., in the University of Colorado Cancer Center DNA Sequencing and Analysis Core, supported by the NIH/National Cancer Institute Cancer Core Support Grant (P30 CA046934).

References

1. Singh M, Spoelstra NS, Jean A, et al. ZEB1 expression in type I vs type II endometrial cancers: a marker of aggressive disease. *Mod Pathol* 2008; 21:912–23.
2. Spoelstra NS, Manning NG, Higashi Y, et al. The transcription factor ZEB1 is aberrantly expressed in aggressive uterine cancers. *Cancer Res* 2006;66:3893–902.
3. Eger A, Aigner K, Sonderegger S, et al. δ EF1 is a transcriptional repressor of E-cadherin and regulates epithelial plasticity in breast cancer cells. *Oncogene* 2005;24:2375–85.
4. Guaita S, Puig I, Franci C, et al. Snail induction of epithelial to mesenchymal transition in tumor cells is accompanied by MUC1 repression and ZEB1 expression. *J Biol Chem* 2002;277:39209–16.
5. Ohira T, Gemmill RM, Ferguson K, et al. WNT7a induces E-cadherin in lung cancer cells. *Proc Natl Acad Sci U S A* 2003;100:10429–34.
6. Aigner K, Dampier B, Descovich L, et al. The transcription factor ZEB1 (δ EF1) promotes tumour cell dedifferentiation by repressing master regulators of epithelial polarity. *Oncogene* 2007;26:6979–88.
7. Aigner K, Descovich L, Mikula M, et al. The transcription factor ZEB1 (δ EF1) represses plakophilin 3 during human cancer progression. *FEBS Lett* 2007;581:1617–24.
8. Horn LC, Meinel A, Handzel R, Einkenel J. Histopathology of endometrial hyperplasia and endometrial carcinoma: an update. *Ann Diagn Pathol* 2007;11:297–311.
9. Ryan AJ, Susil B, Jobling TW, Oehler MK. Endometrial cancer. *Cell Tissue Res* 2005;322:53–61.
10. Kurman RJ, Shih le M. Pathogenesis of ovarian cancer: lessons from morphology and molecular biology and their clinical implications. *Int J Gynecol Pathol* 2008;27:151–60.
11. McCluggage WG. My approach to and thoughts on the typing of ovarian carcinomas. *J Clin Pathol* 2008;61:152–63.
12. Shih le M, Kurman RJ. Ovarian tumorigenesis: a proposed model based on morphological and molecular genetic analysis. *Am J Pathol* 2004;164:1511–8.
13. Zhang W, Dahlberg JE, Tam W. MicroRNAs in tumorigenesis: a primer. *Am J Pathol* 2007;171:728–38.
14. Kent OA, Mendell JT. A small piece in the cancer puzzle: microRNAs as tumor suppressors and oncogenes. *Oncogene* 2006;25:6188–96.
15. Calin GA, Liu CG, Sevignani C, et al. MicroRNA profiling reveals distinct signatures in B cell chronic lymphocytic leukemias. *Proc Natl Acad Sci U S A* 2004;101:11755–60.
16. Hurteau GJ, Carlson JA, Spivack SD, Brock GJ. Overexpression of the microRNA hsa-miR-200c leads to reduced expression of transcription factor 8 and increased expression of E-cadherin. *Cancer Res* 2007;67:7972–6.
17. Gregory PA, Bert AG, Paterson EL, et al. The miR-200 family and miR-205 regulate epithelial to mesenchymal transition by targeting ZEB1 and SIP1. *Nat Cell Biol* 2008;10:593–601.
18. Park SM, Gaur AB, Lengyel E, Peter ME. The miR-200 family determines the epithelial phenotype of cancer cells by targeting the E-cadherin repressors ZEB1 and ZEB2. *Genes Dev* 2008;22:894–907.
19. Albitar L, Pickett G, Morgan M, Davies S, Leslie KK. Models representing type I and type II human endometrial cancers: Ishikawa H and Hec50c cells. *Gynecol Oncol* 2007;106:52–64.
20. Kyo S, Nakamura M, Kiyono T, et al. Successful immortalization of endometrial glandular cells with normal structural and functional characteristics. *Am J Pathol* 2003;163:2259–69.
21. Chapdelaine P, Kang J, Boucher-Kovalik S, et al. Decidualization and maintenance of a functional prostaglandin system in human endometrial cell lines following transformation with SV40 large T antigen. *Mol Hum Reprod* 2006;12:309–19.
22. Wiesen KM, Xia S, Yang CP, Horwitz SB. Wild-type class I β -tubulin sensitizes Taxol-resistant breast adenocarcinoma cells harboring a β -tubulin mutation. *Cancer Lett* 2007;257:227–35.
23. Pillai RS, Bhattacharyya SN, Artus CG, et al. Inhibition of translational initiation by Let-7 MicroRNA in human cells. *Science* 2005;309:1573–6.
24. Place RF, Li LC, Pookot D, Noonan EJ, Dahiya R. MicroRNA-373 induces expression of genes with complementary promoter sequences. *Proc Natl Acad Sci U S A* 2008;105:1608–13.
25. Cleary MP, Juneja SC, Phillips FC, et al. Leptin receptor-deficient MMTV-TGF- α /Lepr(db)Lepr(db) female mice do not develop oncogene-induced mammary tumors. *Exp Biol Med (Maywood)* 2004;229:182–93.
26. Garofalo C, Koda M, Cascio S, et al. Increased expression of leptin and the leptin receptor as a marker of breast cancer progression: possible role of obesity-related stimuli. *Clin Cancer Res* 2006;12:1447–53.
27. Miyoshi Y, Funahashi T, Tanaka S, et al. High expression of leptin receptor mRNA in breast cancer tissue predicts poor prognosis for patients with high, but not low, serum leptin levels. *Int J Cancer* 2006; 118:1414–9.
28. Geiger TR, Peeper DS. Critical role for TrkB kinase function in anikis suppression, tumorigenesis, and metastasis. *Cancer Res* 2007;67: 6221–9.
29. Chenard CA, Richard S. New implications for the QUAKING RNA binding protein in human disease. *J Neurosci Res* 2008;86:233–42.
30. Galarneau A, Richard S. Target RNA motif and target mRNAs of the Quaking STAR protein. *Nat Struct Mol Biol* 2005;12:691–8.
31. Harding MA, Theodorescu D. RhoGDI2: a new metastasis suppressor gene: discovery and clinical translation. *Urol Oncol* 2007;25:401–6.
32. Conover JC, Doetsch F, Garcia-Verdugo JM, et al. Disruption of Eph/ephrin signaling affects migration and proliferation in the adult subventricular zone. *Nat Neurosci* 2000;3:1091–7.
33. Chumley MJ, Catchpole T, Silvany RE, Kernie SG, Henkemeyer M. EphB receptors regulate stem/progenitor cell proliferation, migration, and polarity during hippocampal neurogenesis. *J Neurosci* 2007;27: 13481–90.
34. Erler JT, Bennewith KL, Nicolau M, et al. Lysyl oxidase is essential for hypoxia-induced metastasis. *Nature* 2006;440:1222–6.
35. Erler JT, Giaccia AJ. Lysyl oxidase mediates hypoxic control of metastasis. *Cancer Res* 2006;66:10238–41.
36. Psaila B, Kaplan RN, Port ER, Lyden D. Priming the “soil” for breast cancer metastasis: the pre-metastatic niche. *Breast Dis* 2006;26:65–74.
37. Pusztai L. Markers predicting clinical benefit in breast cancer from microtubule-targeting agents. *Ann Oncol* 2007;18 Suppl 12:xii15–20.
38. Seve P, Dumontet C. Is class III β -tubulin a predictive factor in patients receiving tubulin-binding agents? *Lancet Oncol* 2008;9:168–75.
39. Paradiso A, Mangia A, Chiriatti A, et al. Biomarkers predictive for clinical efficacy of Taxol-based chemotherapy in advanced breast cancer. *Ann Oncol* 2005;16 Suppl 4:iv14–9.
40. Tommasi S, Mangia A, Lacalamita R, et al. Cytoskeleton and paclitaxel sensitivity in breast cancer: the role of β -tubulins. *Int J Cancer* 2007; 120:2078–85.
41. Kavallaris M, Annereau JP, Barret JM. Potential mechanisms of resistance to microtubule inhibitors. *Semin Oncol* 2008;35:S22–7.
42. Kavallaris M, Kuo DY, Burkhart CA, et al. Taxol-resistant epithelial ovarian tumors are associated with altered expression of specific β -tubulin isoforms. *J Clin Invest* 1997;100:1282–93.
43. Mozzetti S, Ferlini C, Concolino P, et al. Class III β -tubulin overexpression is a prominent mechanism of paclitaxel resistance in ovarian cancer patients. *Clin Cancer Res* 2005;11:298–305.
44. Umezū T, Shibata K, Kajiyama H, et al. Taxol resistance among the different histological subtypes of ovarian cancer may be associated with the expression of class III β -tubulin. *Int J Gynecol Pathol* 2008; 27:207–12.

Molecular Cancer Therapeutics

MicroRNA-200c mitigates invasiveness and restores sensitivity to microtubule-targeting chemotherapeutic agents

Dawn R. Cochrane, Nicole S. Spoelstra, Erin N. Howe, et al.

Mol Cancer Ther 2009;8:1055-1066. Published OnlineFirst May 12, 2009.

Updated version Access the most recent version of this article at:
doi:[10.1158/1535-7163.MCT-08-1046](https://doi.org/10.1158/1535-7163.MCT-08-1046)

Supplementary Material Access the most recent supplemental material at:
<http://mct.aacrjournals.org/content/suppl/2009/05/05/1535-7163.MCT-08-1046.DC1>

Cited articles This article cites 44 articles, 14 of which you can access for free at:
<http://mct.aacrjournals.org/content/8/5/1055.full#ref-list-1>

Citing articles This article has been cited by 11 HighWire-hosted articles. Access the articles at:
<http://mct.aacrjournals.org/content/8/5/1055.full#related-urls>

E-mail alerts [Sign up to receive free email-alerts](#) related to this article or journal.

Reprints and Subscriptions To order reprints of this article or to subscribe to the journal, contact the AACR Publications Department at pubs@aacr.org.

Permissions To request permission to re-use all or part of this article, use this link
<http://mct.aacrjournals.org/content/8/5/1055>.
Click on "Request Permissions" which will take you to the Copyright Clearance Center's (CCC) Rightslink site.